Dalton Transactions

Accepted Manuscript

This is an *Accepted Manuscript*, which has been through the Royal Society of Chemistry peer review process and has been accepted for publication.

Accepted Manuscripts are published online shortly after acceptance, before technical editing, formatting and proof reading. Using this free service, authors can make their results available to the community, in citable form, before we publish the edited article. We will replace this *Accepted Manuscript* with the edited and formatted *Advance Article* as soon as it is available.

You can find more information about *Accepted Manuscripts* in the Information for Authors.

Please note that technical editing may introduce minor changes to the text and/or graphics, which may alter content. The journal's standard Terms & Conditions and the Ethical guidelines still apply. In no event shall the Royal Society of Chemistry be held responsible for any errors or omissions in this *Accepted Manuscript* or any consequences arising from the use of any information it contains.

ROYAL SOCIETY OF CHEMISTRY

www.rsc.org/dalton

Journal Name
Dalton Transaction

Dalton Transactions

Dynamic Article Links▶

Cite this: DOI: 10.1039/c0xx00000x

www.rsc.org/xxxxxx

ARTICLE TYPE

Facile Synthesis and Photoluminescence Spectroscopy of 3D-Triangular GaN Nano Prism Islands

Mukesh Kumar[a], S.K. Pasha[a], Shibin Krishna T.C.[a] Avanish Pratap Singh[b], Pawan Kumar[c], Bipin Kumar Gupta[c],* and Govind Gupta[a],*

Received (in XXX, XXX) XthXXXXXXXXX 20XX, Accepted Xth XXXXXXXXX 20XX
DOI: 10.1039/b000000x

We report the strategy for fabrication of 3D triangular GaN nano prism islands (TGNPI) grown on Ga/Si(553) substrate at low temperature by N_2^+ ions implantation using sputtering gun technique. The annealing of Ga/Si(553) (600°C) followed by nitridation (2 keV) shows the formation of high quality GaN TGNPI cross-section. TGNPI morphology has been confirmed by Atomic force microscopy. Furthermore, these nanoprism islands exhibit prominent ultra-violet luminescence peaking at 366 nm upon 325 nm excitation wavelength along with low intensity of yellow luminescence broad peak at 545nm which characterizes low defects density TGNPI. Furthermore, the time-resolved spectroscopy of luminescent TGNPI in nanoseconds promises its futuristic applications in next generation UV-based sensors as well as many portable optoelectronic devices.

1. Introduction

Recently, 3D triangular gallium nitride (GaN) nano prism island (TGNPI) offers seminal role in optically active nanoscale material for several optoelectronic and optical sensing device applications.[1, 2] For example, GaN nano prism island based devices can be grown directly on silicon substrates.[1] Fundamentally, GaN, constituent of III-V family, is a wide band gap nitride semiconductor with direct band gap of 3.39 eV at room temperature.[3] GaN has a lower work function of 4.1eV, high thermal stability, mechanical hardness, chemical stability with a lower electron affinity of 2.7-3.3 eV.[4] Therefore, GaN may be a promising material for many optoelectronic devices such as laser diode, light-emitting diode, UV-based sensors and high-power electronics applications. Nowadays, 3D islands formed using heteroepitaxy technique; in primarily growth stages have very significant influences on film qualities and it is subject of interest to explore their optical properties. The stringent criteria for high quality films have motivated intense research interest on the island shaping and shape variations for developing high performance future miniature devices.[1, 5] However, the island shaping is critically dependent on substrates orientation and growth conditions. Currently, the topic of 3D shaped island morphologies of nano-crystalline have become an important aspect of research due to the technological significance as well as the potential applications in the fabrication of 3D ordered arrays of nanoscale smart optoelectronic devices.[5] For example, the photoluminescence of GaN nanostructures in the ultraviolet (UV) has been observed to be dependent on the growth direction of GaN.[6] For successful design of the device, the better growth quality with prominent nanostructure is highly desired. A variety of techniques for GaN growth have been employed including the extensively used techniques such as vapour-liquid-solid (VLS)[7, 8], metal-organic chemical vapour deposition (MOCVD)[9] and molecular beam epitaxy (MBE).[7, 10]

In the present investigation, the sputtering gun technique has been employed for GaN synthesis which is relatively inexpensive and simpler technique that offers the possibility of growth at lower substrate temperature.[11, 12] This technique has different growth mechanism than the evaporation depositions where substances are deposited on or forced into lattice without chemical reaction. Generally, the temperature of metal target is a key parameter for metal nitride formation. For the growth of shape oriented nanostructures, the catalyst is used for the growth of various types of metal nitride nanostructures such as nanocolumn or nanorod. The existence of catalyst in the metal nitride nanostructure serves as an impurity that could be undesirable for device fabrication. The catalyst free growth of nanostructures using sputtering gun technique can be possible by pre-annealing of metal/substrate system such as gallium on suitable substrate and discussed in present investigations.

Dalton Transactions Accepted Manuscript

In order to explore spectroscopic properties, the photoluminescence (PL) is a direct optical tool to probe the intrinsic material properties (electronic energy band structure, shape, strain, surface defect etc.), the sensitivity of the nanostructure to the environment changes. The probability of a material to exhibits the intrinsic band structure and other internal/external defects[13]. We have performed steady state and time-resolved photoluminescence (TRPL) measurements to determine the high quality, strain free material. The photoluminescence emission of GaN is mainly due to either near band gap excitonic emission or due to structural defects as well as presence of internal/external impurities. In some of previous reports, the observed PL spectra are attributed due to presence of the defect induced impurities of sample that are involved during the synthesis process like other synthesis of BN[14]. Normally, impurities associated defects and donor acceptor states may be formed within the GaN band gap, leading to the PL in the visible region (yellow emission). Therefore, it is of fundamental interest to explore and analyse the structure to ensure the quality of GaN film for thin film based devices. TRPL is a non-destructive and commanding technique generally used for optical characterisation of semiconductors to explore their transition behaviour. The PL decay life-time is an important parameter related to the quality of the material and its performance which can be studied using TRPL spectroscopy and is relevant particularly to applications such as optical displays, optical sensors and clinical diagnostic and bio-imaging etc.[14]

Herein, in this report, we have successfully synthesized 3D TGNPI from Ga/Si(553) system at low growth temperature by N_2^+ ions implantation using sputtering gun technique. Fabrication of 3D triangular GaN nano prism islands with detailed spectroscopy merely reported in any literature as per best of our knowledge which is the main novelty of our findings. TGNPI has been characterized by several techniques such as XRD (x-ray diffraction), SEM (scanning electron microscopy), Raman, FTIR (Fourier transform infrared spectroscopy), AFM (atomic force microscopy) and photoluminescence spectroscopy. Addition to this, we have also demonstrated the time-resolved spectroscopy of luminescent TGNPI in nanoseconds regimes which is highly desired for GaN based high performance devices and ultra-fast optical sensor.

2. Experimental

2.1 Growth of TGNPI

Prior to the formation of GaN, the kinetically controlled growth of few monolayer Ga metal on high index stepped Si (553) surface at room temperature along with residual thermal desorption has been reported earlier by our group[15]. In the present investigation, the growth of GaN is performed by pre-depositing Ga on Si (553) surface followed by nitridation, where initial stable (111) 6x6+modified (331) superstructural phases was observed. This was assumed to act as nucleation sites for the growth of GaN nanostructures via nitridation. During the nitridation process, it is difficult to capture an intermediate superstructural phenomenon which is proposed in the present investigation.

2.2 Characterization

The formation of TGNPI on stepped Si (553) surface has been carried out in an UHV system (Varian-VT112) equipped with Auger electron spectroscopy (AES), and low energy electron diffraction (LEED), sputtering gun and residual gas analyzer (RGA) operated at a base pressure of $5x10^{-11}$ torr. Modified Shiraki process was adopted for ex-situ cleaning of the sample (p-type, B-doped, resistivity 0.5 Ω/cm, size ~20x8x0.35 mm^3) followed by in-situ annealing at 600°C (~6 hours), flashing at 1100°C (to remove the native oxide layers) and slowly cooling to room temperature (RT). The sample temperature was monitored using W-Re (5%-25%) thermocouple fixed on the clamp. Homemade tantalum Knudsen cell was used to evaporate Ga metal (CERAC, 99.999%) by circulating the current to control the evaporated material flux. Subsequent nitridation of the deposited Ga layers was carried out using sputter ion gun by 2-keV low energy nitrogen (N_2^+) ion (LENI) at different substrate temperatures (RT-650°C) leading to the formation of GaN compound. However, for temperature > 600 ^{o}C the desorption rate of Ga was quite high so the amount of GaN formation was significantly reduced. The gross structure analysis as well as the crystalline nature all the GaN nanostructures (grown at RT, 450, 650°C) were carried out by PANalytical high-resolution x-ray diffraction (HR-XRD) instrument using CuKα radiation (λ= 1.5405Å) in scattering range (2θ) of 30-50° with a scan rate of 0.02°/sec and slit width of 0.1mm. Fourier transform infrared (FTIR) spectra have been recorded on Nicolet 5700 in transmission mode and wave number range 400-1000 cm^{-1} with a resolution of 4cm^{-1}performing 32 scans. Raman studies were carried out using RenishawinVia Raman spectrometer with an excitation source of 514.5 nm wavelength. The XPS measurements of GaN/Si (553) were performed on Omicron-multiprobe surface analysis system using $MgK_α$ X-ray source (1253.6 eV). Core level (CL) spectra of Ga (3d), N (1s) have been fitted by using Shirley background and Gaussian line shape. The position of valence band maximum was calculated by extrapolating a linear fit to the leading edge of the fitted valence band spectra. Binding energies were calibrated against the binding energy of the standard C (1s) peak at 284.6 eV as well as gold has been deposited on a small portion of the sample and has been taken as a standard in order to take care of the any kind of shifts due to charging and other factors. Further, the morphology of as-grown GaN nanostructures (that is, confinement of carriers in low dimensional structures) with associated defects can affect the material properties. Therefore, the GaN nanostructures morphology and the associated defects can be effectively probed using AFM and PL measurements. The surface morphology of the GaN/ Si (553) surface was analysed by NT-MDT Solver Pro-Atomic Force Microscopy (AFM). PL characterization was carried out using luminescence spectrometer (Edinburgh, FLSP-920) with xenon flash lamp as the source of excitation as well as TRPL was recorded using a time correlated single photon counting technique with instrument (Edinburgh, FLSP-920) equipped with steady state and time-resolved luminescence spectrometer, using a picoseconds He-Cd laser (325 nm) as the source of excitation.

This journal is © The Royal Society of Chemistry [year]

Dalton Transactions Accepted Manuscript

3. Results and discussion

TGNPI were grown on stepped Si (553) surface by depositing Ga metal followed by energetic N_2^+ion interaction as shown in Figure 1(a). The actual set up used for the synthesis of GaN TGNPI is shown in supporting information (see Figure S1). In the 2D (two dimensional) TGNPI shaping, the formation of triangular islands is proposed to form on either fcc (111) or hcp (001) which is further confirmed by gross structural analysis. The self organization of 3D-island occurred during the in-situ sputtering/annealing process of GaN prepared on Si (553) substrate. The distinct triangular islands are supposed to be uniform and aligned with sharp triangular corner which is further evidenced by actual AFM micrograph. The origin of triangular shape TGNPI can be explained via simple technique: during the sputtering process, initially GaN formed due to energetic nitridation by nitrogen ions which first diffuses through the deposited Ga surface and segregated on the surface of gallium deposited layer which convert into nuclei centres of GaN prismatic basal plane nuclei. As we know, that the process is continuous where sputtering and annealing simultaneously present under nitrogen ion environment. Afterward the unstable molecule of GaN further decomposes and reconstructs to form a prismatic basal plane at different nuclei through gas phase transport to form newly shaped islands. The adatoms attached to the island edges may also effectively migrate along the island peripheries specially, when the island size is small (~ 100 nm) and the Ga adatoms diffusion is enhanced. Therefore, the island shaping is determined by the competition between the growth rate of island edge facet via decomposition and re-constructed Ga adatom. The cross section view of wurtzite GaN phase which is the basic build block of TGNPI has demonstrated in Figure 1(b).

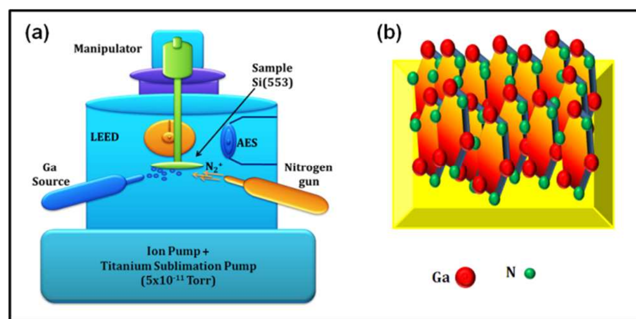

Figure 1(a) Schematic representation of growth system equipped with Auger electron spectroscopy, low energy electron diffraction, Ga source and low energy nitrogen gun. **(b)** Cross sectional view of wurtzite GaN showing the hexagonal structure of GaN.

The HRXRD analysis is performed to examine the crystal structure and phase purity of GaN nanostructure grown under different conditions (RT, 450 and 600ºC). Figure 2 (a) exhibits hexagonal wurtzite GaN reflection (100), (002), (101) and (102) peaks at RT. For, 450 and 600ºC, the formation of TGNPI achieved where (100) and (101) plane act as basal plane for TGNPI hexagonal wurtzite phase of GaN. The (002) plane is dominant to other planes in this case due to TGNPI grow along (002) axis. The estimated crystal structure lattice parameters for TGNPI grown at 600ºC are a=(3.1600±0.0023) Å and c=(5.2000 ± 0.0019) Å. These values are in good agreement with those listed in standard JCPDS card for wurtzite GaN (card No. 50-0792). No cubic and other impurity phase of GaN was observed. Figure 2(b) exhibits the Raman spectra of GaN nanostructure (RT, 450 and 600ºC) over a wave number range of 500-800 cm^{-1} on Si (553) substrate at room temperature. The main GaN phonon modes are A_1+E_1+2B_1+2E_2, where A_1 (LO), E_1 (TO), E_2 (High) and Low modes are Raman active and the 2B_1 (silent modes) are inactive.[16] The observed peaks at 572, 580 and 753 cm^{-1} may be E1 (TO), E_2 (High) and A_1 (LO) modes respectively as shown in Figure 2 (b). For TGNPI grown at 600 ºC, a shift of 2cm^{-1} towards lower wave number is observed which indicates the TGNPI structure contain tensile stress of 0.4GPa. Figure 2(c) shows the FTIR spectra with a single peak of GaN vibration which appears at 556 cm^{-1}due to Ga-N stretching vibration[17] in the hexagonal type GaN crystal for samples grown at RT, 450 and 600ºC. Figure 2(d) exhibits the SEM micrograph of TGNPI (600ºC) where it can be easily seen the individual 3D-triangular prism morphology having basal plane of dimension about 80nm.

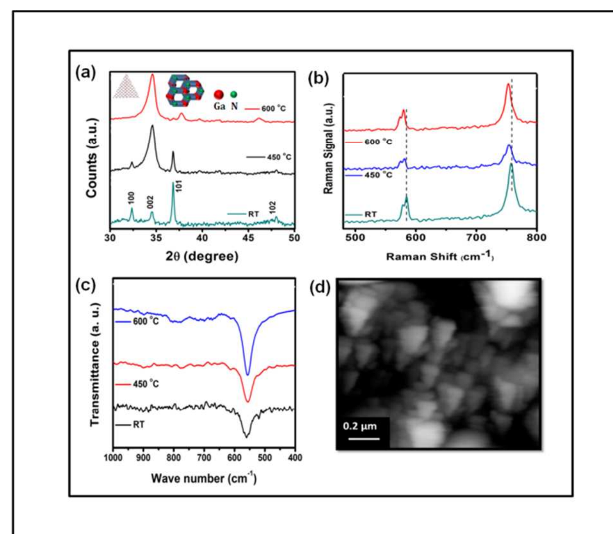

Figure 2(a) XRD pattern of GaN grown at RT, 450 and 600°C while left inset shows the growth model for TGNPI and right inset shows the cross-sectional view of wurtzite phase, **(b)** exhibits the Raman spectrum at different growth temperature, **(c)** FTIR spectra of GaN at different growth temperature (**d)** SEM micrograph of TGNPI .

The structural morphology of the GaN nanostructures using 2 keV-LENI has been investigated by AFM technique. The AFM scans illustrate the surface texture of the GaN/Si (553) system where the surface consists of large number of distributed symmetrical GaN nanostructures grown at RT, 450 and 600ºC (Figure 3). For RT, the structure without the triangular morphology has been observed as shown in Figure 3(a). For 450ºC partially nucleated triangular nanostructures were achieved as shown in Figure 3(b). Further, when we employed 600 ºC growth temperatures, uniformly developed controlled triangular nano prism islands were achieved as shown in details Figure 3(c). The sequential low resolution AFM images are also shown in Figure S2 and S3 which clearly demonstrates the

Dalton Transactions Accepted Manuscript

TGNPI morphology. Figure 3(d) represents the 3D image of the GaN island exhibits the distinct and smooth sidewall faceting of TGNPI.

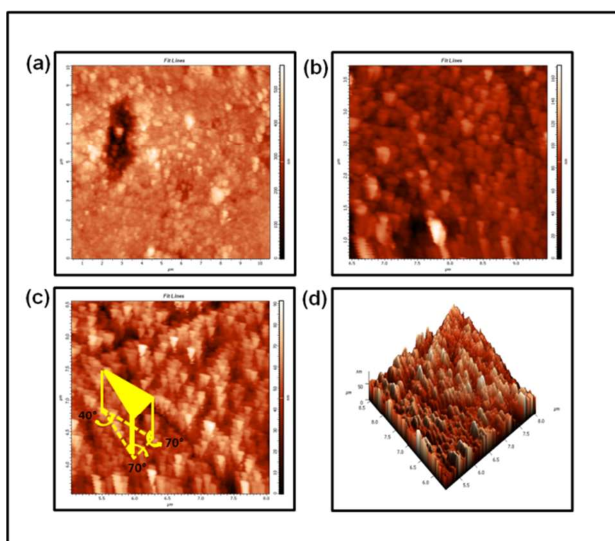

Figure 3 AFM micrograph of GaN nanostructures grown at **(a)** RT **(b)** 450 °C **(c)** 600 °C and **(d)** 3D view of TGNPI structure grown at 600 °C.

These GaN TGNPI consists of faceted surface enclosed by three sidewalls results the triangular cross-section. Although it is difficult to determine the detailed conFiguration of the triangular nanostructures due to the well-known convolution effect of AFM tips, and the protrusion of the nanostructures were several tens of nanometers. The average size of these GaN nanostructures can be estimated by calculating the average triangle size <l >, which can be defined as

$$<l>=1/n^{1/2} \quad (1)$$

where n is the total number of triangle per unit area.[17] The average size of the triangular nanostructures < l > is found to be ~ 75 nm. Thus, these structures can be referred as triangular GaN nano-prism islands (TGNPI). The formation of uniform symmetrical TGNPI were suppose to be resulted from the annealing of Ga/Si(553) system. On annealing at 600°C temperature, the Ga develop into thermally stable islands with induced super structural phase {(111) 6x6+modified (331)}[2] on the Si (553) substrate[15] and serve as a nucleation sites for TGNP growth. The measured internal angles of the TGNPI were found to be around 40°, 70°, and 70° where the slight variations in measurements may be there due to the extraction of on-screen data. It indicates that the cross-section of a TGNPI would be an isosceles rather than an equilateral triangle that is, the observation of these triangular cross-sections is not a result of viewing along the six-fold crystallographic symmetry axis which is generally observed for hexagonal wurtzite structure. Instead, the isosceles triangular cross-section is a manifestation of the two-fold symmetry. The unique nanoscale isosceles triangle of GaN might also lead to interesting carrier-confinement effects at the triangle vertices.

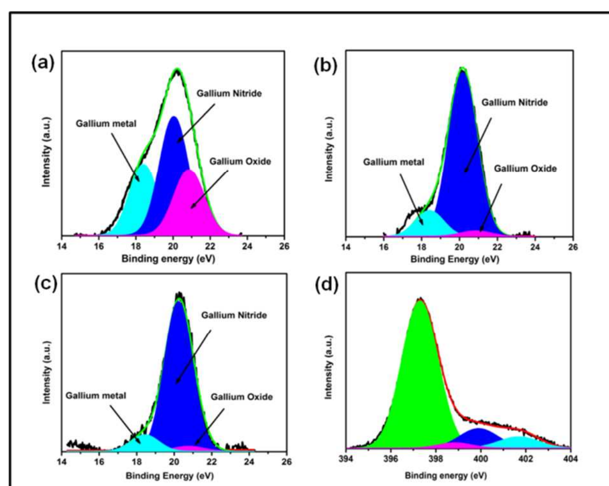

Figure 4 Deconvoluted XPS core level spectra of Ga (3d) of GaN/Si(553) surface using 2keV nitrogen ions at various temperatures **(a)** RT, **(b)** 450°C, **(c)** 600°C and **(d)** N(1s) spectra for GaN/Si(553) formed at 600°C using 2keV nitrogen ions.

The deconvoluted XPS core level spectra (CLS) of Ga($3d_{5/2}$) of GaN using 2 keV-LENI at different substrate temperatures is shown in Figure 4(a-c). Deconvoluted Ga ($3d_{5/2}$) CL spectra (Figure 4 (a-c)) comprised of three peaks, main peak at binding energy (BE) 20.2 eV and two other smaller peaks at BE 18.4 eV and 20.9 eV. The component of BE at 18.4 eV signifies the presence of metallic Gallium adlayer (Ga-Ga) in the sample[1, 18]. Further, a chemical shift (1.4-1.5eV) in the BE position of dominating peak to the BE of metallic Gallium peak has been observed in deconvoluted Ga ($3d_{5/2}$) CL spectra. The shift in the BE position is caused by subtle change of the inner electron binding energy due to different chemical environments which arises from the difference between atomic valences. Thus the presence of peak at 20.2eV confirms the bonding between Ga and N atoms and described the formation of GaN bond[1, 18] .The occurrence of metallic Ga in Ga ($3d_{5/2}$) CL spectra indicate the presence of Ga atoms which did not interact with N species. Furthermore, there is a strong tendency for GaN surfaces to be stabilized by Ga atoms in the surface layers due to the small lattice constant and high anion-anion bond strength for GaN compared to those of conventional III-V semiconductors[19]. A small peak at BE of 20.9eV could be attributed to Ga-O bond formation in GaN since as-grown GaN samples were exposed to air during ex-situ transfer to the XPS analysis and the presence metallic Ga at the GaN surface also make the surface more susceptible for the oxidation. Figure 4 (a) demonstrate the deconvoluted Ga ($3d_{5/2}$) CL spectra for GaN using 2keV-LENI at RT. The ratio of area under the peaks of GaN/Ga ($A_{GaN/Ga}$) was found to be 1.7 which reveals the low extant of interaction of Ga atoms with N-ions at RT. Figure 4 (b) shows the formation of GaN using 2keV-LENI at 450°C where the significant reduction in the contribution of Ga-Ga and Ga-O was observed. Further the value of $A_{GaN/Ga}$ found to be 6.4, which signifies the higher nitridation at 450°C than RT. Since the atomic diffusion is the characteristics of thermal process. Therefore, annealing of substrate at 450°C provides thermal energy to the Ga atoms and

Dalton Transactions Accepted Manuscript

 This journal is © The Royal Society of Chemistry [year]

the implanted light atoms that are mobile at elevated temperature can diffuse into the mother lattice. Also, there is a less probability thermal decomposition of GaN at low temperature. These considerations may be the reason for higher nitridation at 450°C than RT. On further increasing, the nitridation temperature to 600°C, the value of $A_{GaN/Ga}$ increased to 9.8 which indicate significant interaction of Ga atoms with N-ions. On further increasing the nitridation temperature (>600°C) a significant reduction in the Ga coverage has been observed due to the desorption of Ga from Si (553) surface. XPS CL spectra analysis revealed that 2 keV-LENI at 600°C provide required energy for the high quality growth of GaN. Further, the contribution of Ga in Ga-rich GaN can be control by optimized the substrate temperature. The deconvoluted CL-N (1s) spectra has also been shown for 2 keV-LENI at 600°C which contain peak at 397.0 eV (GaN) along with three small peaks at 399 eV (N-O-Ga), 400 eV (N-H) and 401.7eV (N-C). The peaks corresponding to N-H & N-C components might have occurred due to surface H- and C-adsorption, during ex-situ sample transfer process.

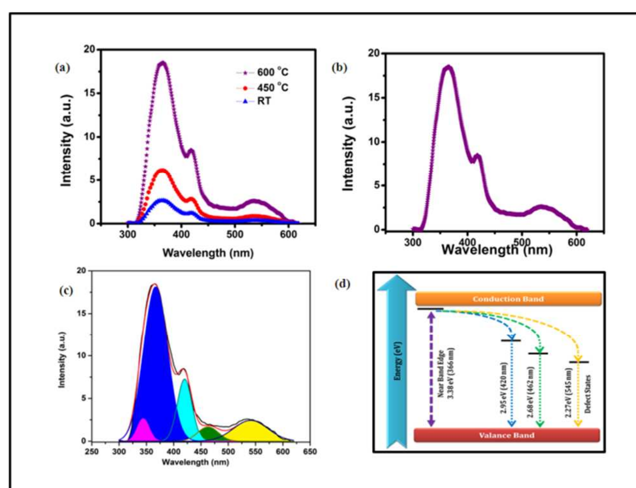

Figure 5 (a) shows the photoluminescence emission spectra of GaN grown at different temperatures **(b)** PL emission spectrum of TGNPI grown at 600°C. **(c)** Deconvoluted Gaussian residuals peaks of TGNPI and **(d)** proposed energy level diagram based on Gaussian fitting.

The energy structure of GaN/Si(553) was identified by valence band (VB) spectra. The corresponding VB spectra are shown in Figure S4 (a-c) (supporting information). There were two dominant structures except the core level Ga (3d) peak, in the valence band spectra. The Gaussian fitted peaks of these two structures were centered at BE of 5.7 eV and 10 e V. The 5.7 eV feature is mainly due to nitrogen p-derived, and the peak at 10 eV is associated with hybridized Ga (s) and N (p) states and the location of these two maxima agree well with the reported values and major density of states (DOS) features predicted in band structure calculations.[20, 21] The RT grown GaN Figure S4 (a) as well as 450°C grown samples Figure S4 (b) have slight reduced intensity of nitrogen p-derived structure than the feature associated with hybridized Ga (s) and N(p) states. While, these features have comparable intensity for 600°C grown sample Figure S4 (c). As the Ga-component was different in different conditions grown GaN samples and reduce with increase in growth temperature up to 600°C as shown in Figures S4(a-c). It suggests that the low temperature grown GaN sample exhibit more nitrogen depleted surface which changes the line-shape of the valence band. Therefore, the feature associated with hybridized Ga (s) and N(p) states remains intact, while the nitrogen p-derived structure reduced in intensity with higher nitrogen depleted surface in GaN which is further evident by photoluminescence spectroscopy where PL intensity of TGNPI is higher in compared to RT & 450 grown samples.. The tail of valence band spectra shows the existence of surface states below the unidentified accurate position of VB maximum (VBM) where some energy states lying below the zero binding energy. If a significant number of occupied states in the band gap of GaN exist at the surface, photoemission could occur from these states and would cause the valence band leading edge to appear falsely and makes it difficult to determine the position of VBM. These observed states, exist below the VBM, can result from various factors such as small gallium component in the GaN sample, differences in film/surface preparation, defects, strain and contaminants. It is interesting to note that the reported BE values of CL Ga (3d)-VBM for GaN varies in the range of 17.1-18.4 eV and the VBM of clean GaN surfaces located in the 2.4–2.7 eV range below the Fermi level.[22] However, CL-VBM values are independent of the measurement art effects due to existence of surface states.[22, 23] The leading edge of the Gaussian fit peak comes around 2.5 eV Figure S4(c) suggesting the position of VBM and the CL-VBM value to be 17.7 eV.

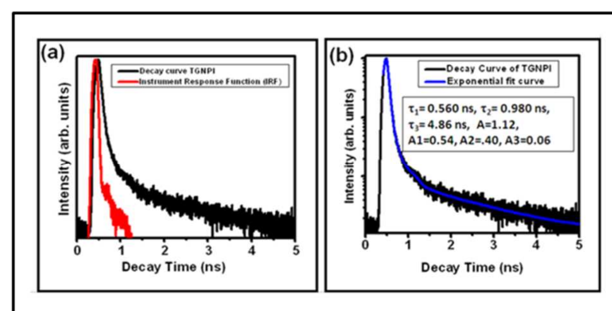

Figure 6(a) shows the TRPL spectrum of the TGNPI upon 366nm emission at 325 nm excitation wavelengths (RT), **(b)** exponential fitted decay curve of TGNPI while inset shows the curve fitting generated parameters.

Being able to visualize the optoelectronic devices on the basis of optical properties of the TGNPI, the photoluminescence studies were carried out. Figure 5(a-c) shows the photoluminescence emission spectrum of GaN nanostructures upon 325nm excitation wavelength at room temperature. Figure 5(a) displays the photoluminescence emission spectra of GaN grown at RT, 450 and 600 °C. The PL results reveal that the intensity of the PL spectrum of TGNPI grown at 600°C is ~ 3 and 7 times higher than 450 and RT grown samples respectively. The observed higher PL intensity in case of TGNPI grown at 600 °C originates due to higher crystallinity achieved which creates more electron and hole for recombination as compared to RT and 450°C grown samples. The availability of the higher electron hole

Dalton Transactions Accepted Manuscript

pair density in GaN nanostructures depends upon the contributions of GaN as well as N-p derivatives which control the recombination process. In the present case, the sample grown at 600°C has less N-p derivative as compared to RT & 450°C. The presence of higher p-derivative quenches the luminescence which can be easily seen in Figure 5(a). The PL results are in good correlation with the observed VB spectra as shown in Figure S4.

In order to explore the detailed mechanism of the photoluminescence phenomena of TGNPI grown at 600°C, we plot the separate PL spectrum of TGNPI grown at 600°C and decovoluated the spectrum which are shown in Figure 5(b) and 5(c). Mainly three dominant Gaussian fit peak structures centred at 366 nm, 420 nm and 545nm have been observed besides the Gaussian residuals peaks around 345 nm and 461 nm as shown in Figure 5 (c). The pronounce peak feature centred at 366 nm **is** corresponds to the near-bandgap emission (NBE) for the GaN where the peak position is characteristics wavelength corresponding to band-edge emission[24]. The contributions to the NBE that result in the broadening of emission peak, can result from the excitons bound to neutral shallow donor impurities, point defects and structural defects such as stacking faults from the bottom interface of the nanostructures[25]. The residual peak feature results from the asymmetry in the PL peak structure that has emission around 345 nm, is blue-shifted relative to the GaN band-edge PL at 366 nm. The possibility of blue shift peak feature may be due to the emission from the triangle vertices of TGNPI where the carriers are confined leading to increased band gap on the basis of quantum confined states. Further, there was a small contribution of Ga at the surface of GaN nanostructures as observed in the XPS spectra as shown in Figure 4 (d), which makes the surface more susceptible to oxidation. Perhaps oxidation of surface that leads to the formation of surface trap states, might also contribute to the emission in the spectral range of the blue-shifted PL. The sub-band-gap emission (SBE) is shown by the dominant sharp peak feature around 420 nm. In case of using silicon substrate, the possible cause for SBE emission may be attributed to the donor-acceptor pair recombination (DAP)[25] due to inter-diffusion of silicon atoms into the GaN nanostructures that has n-type doping behaviour where the acceptor state most likely related to unidentified intrinsic defects in the GaN lattice. In addition, there is a spectral feature consisting of the dominant broad peak structure observed at higher wavelength centred at 545 nm and the residual peak feature around 461 nm. The broad feature around 545 nm, which is yellow luminescence, is a well-known problem in GaN films.[26] These features result from the structural imperfections that are almost six orders of magnitude weaker with respect to the NBE feature which characterized the qualitative superiority of TGNPI with low defects. The band edge as well as defect states associated PL phenomena and their transitions can be easily understand by proposed energy level diagram of TGNPI as shown in Figure 5(d).

Time-resolved photoluminescence spectroscopy (TRPL) is a non destructive and very powerful tool to explore the photoluminescence transition. The PL decay life-time is an important parameter related to the quality of the material and its performance, which can be studied using TRPL spectroscopy, and is relevant particularly to applications such as optical displays, optical sensors, and clinical, diagnostics and bio-imaging. To study the recombination mechanism of the emission, we have carried out time-resolved PL by excitation with a laser line at 325 nm for all samples (grown at RT, 450 and 600°c). It is well established that the TRPL measurements on individually dispersed and as-synthesized GaN nanostructures give PL decay time in the range of ~200 ps to about ~2.7 ns that depend on the temperature and the dimension of the nanostructure.[10] Figure S5 represents decay profile of samples grown at RT, 450 and 600°C. The life-time increases with respect to growth temperature of GaN nanostructures. Time-resolved decay profile basically represents the efficiency of the radiative recombination which is directly proportional to the decay time of the particular transition either it is associated with the impurity or ion and defects. The obtained TRPL results are consistent with acquired PL data. It is clearly evident that the PL intensity is increasing with temperature because the recombination part enhances with respect to temperatures, as a result it can be easy to understand that the life-time quenchs for RT and 450 °C where TGNPI either didn't grow or partially grow. Figure 6 (a) shows the PL decay profile of the TGNPI. The decay was recorded for the TGNPI transition at 366 nm emission obtained at room temperature upon 325nm excitation wavelength of HeCd laser by a time-correlated single-photon counting technique. The life-time data of TGNPI were very well fitted to a triple-exponential function as:

$$I(t) = A_1\exp(-t/\tau_1) + A_2\exp(-t/\tau_2) + A_3\exp(-t/\tau_3) \qquad (2)$$

where τ_1, τ_2 and τ_3 are the decay lifetimes of the luminescence, and A_1, A_2 and A_3 are the weighting parameters. The observed life-times of the TGNPI are τ_1 ~ 0.56 ns,τ_2 ~ 0.96 ns and τ_3~4.86ns as shown in Figure 6 (b).

For triple-exponential decay, the average decay time (τ_{av}), which is determined by the following equation

$$\tau_{av} = \frac{A_1\tau_1^2 + A_2\tau_2^2 + A_3\tau_3^2}{A_1\tau_1 + A_2\tau_2 + A_3\tau_3} \qquad (3)$$

The average PL decay time for TGNPI is calculated as τ_{av} ~ 2 ns. Such decay time compare favorably with the PL decay time and carrier life-times observed in high quality bulk GaN threading dislocations densities at below $10^6 cm^{-2}$.[27, 28] The obtained time-resolved spectroscopy results clearly demonstrate the triple exponential decay curve where the curve fitting generated relative contributions of different weighting parameters A1, A2, A3 are 54%, 40%, 6% respectively. However, it is difficult to designate the energy states, types of defects and defect density which are associated with the obtained weighting parameters. It only reveal that three energy states involved for such transitions correspond to contributions of three decay component in time resolved spectroscopy after exponential curve fitting. The cause of three decay component present in TGNPI is may be due to energy trap in different defect states present in TGNPI structures which was explained in proposed energy level diagram. Thus, the TRPL spectroscopy result suggests that the TGNPI is highly suitable for fast optical UV sensing/switching applications as well as high performance optoelectronic devices.

Dalton Transactions Accepted Manuscript

 This journal is © The Royal Society of Chemistry [year]

4. Conclusions

In conclusions, we have successfully demonstrate the formation of TGNPI GaN from Ga/Si(553) system at low growth temperature by 2 keV-LENI implantation using sputtering gun technique. High quality TGNPI formation is achieved using 2 keV ion energy at substrate temperature 600°C. The morphology of as-grown good quality sample consists of GaN nano-prisms islands with triangular cross-section. These TGNPI have the blue shifted luminescence with a prominent GaN characteristics emission wavelength at 366 nm upon 325nm excitation wavelength. The defects in the TGNPI are observed to be low which is shown by six time lower intensity of defect related PL than the characteristics PL intensity correspond to GaN. Time-resolved spectroscopy of TGNPI reveals that the life-time in nanosecond which promise its potential application for optoelectronic, UV sensor as well as high performance optical switching application at nanoscale.

Notes and references

[a]*Physics of Energy Harvesting Division, CSIR-National Physical Laboratory, Dr K S Krishnan Road, New Delhi-110012, India*
[b]*Polymeric& Soft Materials Section, CSIR-National Physical Laboratory, Dr K S Krishnan Road, New Delhi-110012, India*
[c]*Luminescent Materials and Devices Group, Materials Physics and Engineering Division, CSIR-National Physical Laboratory, Dr K S Krishnan Road, New Delhi-110012, India*

---

* *Corresponding author. Tel.: +91-11-45608403, PRFx: +91-11-4560-9310*
E-mail address: govind@nplindia.org (G),bipinbhu@yahoo.com (B.K.G)

† Electronic Supplementary Information (ESI) available: [details of any supplementary information available should be included here]. See DOI: 10.1039/b000000x/
‡ Footnotes should appear here. These might include comments relevant to but not central to the matter under discussion, limited experimental and spectral data, and crystallographic data.

Acknowledgment

The authors gratefully acknowledge Prof. R. C. Budhani Director, CSIR-NPL, New Delhi, India for constant encouragement and support. The work is supported by CSIR network project TAPSUN (NWP-55) Inorganic Light Emitting Diode Activity.

References:

1. Z. Fang and J. Kang, *J. Phys. Chem. C*, 2007, **111**, 7889-7892.
2. D. V. Dinh and J. H. Yang, *Journal of the Korean Physical Society*, 2009, **55**, 202-206.
3. W. Shan, T. J. Schmidt, R. J. Hauenstein and j. J. Song, *Appl. Phys. Lett.*, 1995, **66**, 3492-3494.
4. D. V. Dinh, S. M. Kang, J. H. Yang, S. W. Kim and D. H. Yoon, *Journal of Crystal Growth*, 2009, **311**, 495-499.
5. M. D. Brubaker, P. T. Blanchard, J. B. Schlager, A. W. Sanders, A. Roshko, S. M. Duff, J. M. Gray, V. M. Bright, N. A. Sanford and K. A. Bertness, *Nano Letters*, 2013, **13**, 374-377.
6. A. H. Chin, T. S. Ahn, H. Li, S. Vaddiraju, C. J. Bardeen, C.-Z. Ning and M. K. Sunkara, *Nano Letters*, 2007, **7**, 626-631.
7. T. Kuykendall, P. J. Pauzauskie, Y. Zhang, J. Goldberger, D. Sirbuly, J. Denlinger and P. Yang, *Nat Mater*, 2004, **3**, 524-528.
8. T. W. George, A. A. Talin, J. W. Donald, J. R. Creighton, L. Elaine, J. A. Richard and A. Ilke, *Nanotechnology*, 2006, **17**, 5773.
9. T. Kuykendall, P. Pauzauskie, S. Lee, Y. Zhang, J. Goldberger and P. Yang, *Nano Lett.*, 2003 **3**, 1063-1066.
10. J. B. Schlager, K. A. Bertness, P. T. Blanchard, L. H. Robins, A. Roshko and N. A. Sanford, *Journal of Applied Physics*, 2008, **103**, 124309-124309-124306.
11. T. Kawabata, F. Okuyamaa and M. Tanemura, *J. Appl. Phys.*, 1991, **69**, 3723-3728.
12. J. A. Taylor, G. M. Lancaster, A. Ignatiev and J. W. Rabalais, *J. Chem. Phys.*, 1978, **68**.
13. B. K. Gupta, V. Shanker, M. Arora and D. Haranath, *Applied Physics Letters*, 2009, **95**, 073115-073115-073113.
14. A. L. M. Reddy, B. K. Gupta, T. N. Narayanan, A. A. Martí, P. M. Ajayan and G. C. Walker, *The Journal of Physical Chemistry C*, 2012, **116**, 12803-12809.
15. M. Kumar, S. K. Pasha and Govind, *Applied Surface Science*, 2013, **283**, 1071-1075.
16. M. Kuball, *Surface and Interface Analysis*, 2001, **31**, 987-999.
17. I. Ermanoskia, C. Kimb, S. P. Keltyb and T. E. Madeya, *Surf. Sci.*, 2005, **596**, 89-97.
18. J. B. Metson, H. J. Trodahl, B. J. Ruck, U. D. Lanke and A. Bittar, *Surface and Interface Analysis*, 2003, **35**, 719-722.
19. T. D. Veal, P. D. C. King, P. H. Jefferson, L. F. J. Piper, C. F. McConville, H. Lu, W. J. Schaff, P. A. Anderson, S. M. Durbin, D. Muto, H. Naoi and Y. Nanishi, *Physical Review B*, 2007, **76**.
20. J. Ma, B. Garni, N. Perkins, W. L. O'Brien, T. F. Kuech and M. G. Lagally, *Appl. Phys. Lett.*, 1996, **69**, 22.
21. M.-Z. Huang and W. Y. Ching, *J. Phys. Chem. Solids*, 1985, **46**.
22. S. W. King, C. Ronning, R. F. Davis, M. C. Benjamin and R. J. Nemanich, *Journal of Applied Physics*, 1998, **84**.
23. X. Xu, X. Liu, Y. Guo, J. Wang, H. Song, S. Yang, H. Wei, Q. Zhu and Z. Wang, *Journal of Applied Physics*, 2010, **107**, 104510.
24. K. M. A. Saron, M. R. Hashim and N. K. Allam, *Journal of Applied Physics*, 2013, **113**, -.
25. F. Furtmayr, M. Vielemeyer, M. Stutzmann, A. Laufer, B. K. Meyer and M. Eickhoff, *J. Appl. Phys.*, 2008, **104**.
26. K. B. Nam, M. L. Nakarmi, J. Y. Lin and H. X. Jiang, *Appl. Phys. Lett.*, 2005, **86**, 222108.
27. T. Malinauskas, R. Aleksiejūnas, K. Jarašiūnas, B. Beaumont, P. Gibart, A. Kakanakova-Georgieva, E. Janzen, D. Gogova, B. Monemar and M. Heuken, *Journal of Crystal Growth*, 2007, **300**, 223-227.
28. S. F. Chichibu, A. Uedono, T. Onuma, T. Sota, B. A. Haskell, S. P. DenBaars, J. S. Speck and S. Nakamura, *Applied Physics Letters*, 2005, **86**, 021914-021914-021913.

Dalton Transactions Accepted Manuscript

Graphical Table of Content

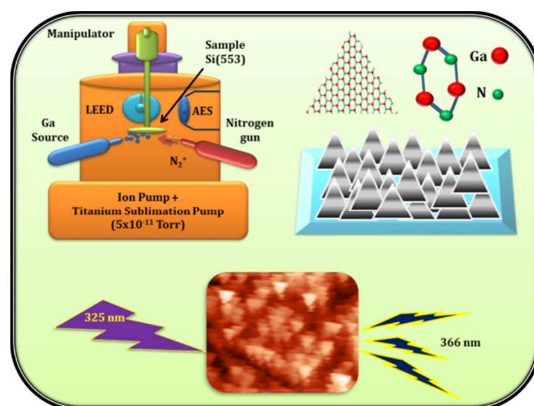

3D-triangular GaN nanoprism islands were grown on Si(553) using sputtering-gun technique. Spectroscopic results promise its futuristic applications in optoelectronic devices.

Dalton Transactions Accepted Manuscript